GEOPHYSICS, VOL. 79, NO. 5 (SEPTEMBER-OCTOBER 2014); P. WB25–WB34, 4 FIGS., 1 TABLE.
10.1190/GEO2013-0417.1

Point-source radiation in attenuative anisotropic media

Bharath Shekar[1] and Ilya Tsvankin[2]

ABSTRACT

Important insights into point-source radiation in attenuative anisotropic media can be gained by applying asymptotic methods. Analytic description of point-source radiation can help in the interpretation of the amplitude-variation-with-offset response and physical-modeling data. We derive the asymptotic Green's function in homogeneous, attenuative, arbitrarily anisotropic media using the steepest-descent method. The saddle-point condition helps describe the behavior of the slowness and group-velocity vectors of the far-field P-wave. Numerical results from the asymptotic analysis compare well with those obtained by the ray-perturbation method for P-waves in transversely isotropic media.

INTRODUCTION

Velocity and attenuation anisotropy significantly influence the radiation pattern of seismic waves excited by a point source. A proper correction for the source directivity can help improve the robustness of amplitude-variation-with-offset (AVO) and attenuation analysis. Point-source radiation in homogeneous anisotropic media has been mostly studied for nonattenuative materials using asymptotic and numerical methods (e.g., Tsvankin and Chesnokov, 1990; Gajewski 1993; Wang and Achenbach, 1994; Červený, 2001). Zhu (2006) presents an analytic and numerical study of point-source radiation in 2D homogeneous, attenuative, transversely isotropic (TI) media. Vavryčuk (2007) derives the asymptotic Green's function for homogeneous, attenuative media with arbitrary anisotropic symmetry by formally extending the results of Wang and Achenbach (1994) obtain for elastic media.

In attenuative media, the Christoffel matrix becomes complex-valued because the stiffnesses acquire an imaginary part (Carcione, 2007; Borcherdt, 2009). Although many results derived for elastic models can be generalized for attenuative media, there are several important differences. In particular, the saddle-point condition involves complex-valued slowness and group-velocity vectors, whose real and imaginary parts can have different directions; hence, the properties of these vectors have to be clearly defined. Here, we present a rigorous derivation of the saddle-point condition and the Green's function in attenuative anisotropic media.

We start by reviewing the definitions of the attenuation coefficient, group velocity, and other key signatures in attenuative media. Then the integral expression for the Green's function in homogeneous attenuative anisotropic media is evaluated by the steepest-descent method. The saddle-point condition is used to study the influence of attenuation on the properties of the far-field P-wave. Finally, we compare the P-wave group-velocity, polarization, and slowness vectors obtained from our asymptotic analysis for TI media with those found from the ray-perturbation theory (Červený and Pšenčík, 2009).

BASIC DEFINITIONS

In attenuative media, the density-normalized stiffness tensor $\tilde{a}_{ijkl}$ is complex-valued (complex quantities are denoted here by the tilde sign on top):

$$\tilde{a}_{ijkl} = a^R_{ijkl} - i a^I_{ijkl}. \tag{1}$$

The components of the frequency-domain displacement vector $\tilde{\mathbf{u}}$ for plane waves propagating in attenuative media can be written as

$$\tilde{u}_i = \tilde{g}_i U e^{i\omega(t - \tilde{\mathbf{p}}\cdot\mathbf{x})}, \tag{2}$$

where $\tilde{\mathbf{g}}$ represents the polarization vector, U is the scalar amplitude, and the slowness vector $\tilde{\mathbf{p}} = \mathbf{p}^R + i\,\mathbf{p}^I$ consists of the real-valued propagation ($\mathbf{p}^R$) and attenuation ($\mathbf{p}^I$) vectors. The wave vector $\tilde{\mathbf{k}}$ is related to the slowness vector by $\tilde{\mathbf{k}} = \omega\,\tilde{\mathbf{p}}$. The orientations of $\mathbf{p}^R$ and $\mathbf{p}^I$ can be different, and the angle between $\mathbf{p}^R$ and $\mathbf{p}^I$ is called the *inhomogeneity (or attenuation) angle* ξ (Červený and Pšenčík,

Manuscript received by the Editor 11 November 2013; revised manuscript received 3 March 2014; published online 16 September 2014.
[1]Formerly Colorado School of Mines, Center for Wave Phenomena, Golden, Colorado, USA; presently Indian Institute of Technology Bombay, Department of Earth Sciences, Mumbai, India. E-mail: bshekar@iitb.ac.in.
[2]Colorado School of Mines, Center for Wave Phenomena, Department of Geophysics, Golden, Colorado, USA. E-mail: ilya@mines.edu.

2005; Behura and Tsvankin, 2009; Tsvankin and Grechka, 2011). Plane waves can satisfy the wave equation for a range of values of ξ, except for those corresponding to certain "forbidden directions" (Krebes and Le, 1994; Červený and Pšenčík, 2005; Carcione, 2007).

For waves excited by point sources, however, the inhomogeneity angle is determined by medium properties and boundary conditions (Zhu, 2006; Vavryčuk, 2007). In reflection/transmission problems for plane waves, the inhomogeneity angle for reflected and transmitted modes is constrained by Snell's law and can reach values of up to 90° (Hearn and Krebes, 1990; Červený, 2007; Behura and Tsvankin, 2009).

Zhu and Tsvankin (2006) define the phase attenuation coefficient $\mathcal{A}^{\mathrm{ph}}$ as

$$\mathcal{A}^{\mathrm{ph}} = \frac{|\mathbf{k}^I|}{|\mathbf{k}^R|}. \tag{3}$$

The angle-dependent phase quality factor Q^{ph} is related to $\mathcal{A}^{\mathrm{ph}}$ by

$$Q^{\mathrm{ph}} = \frac{1}{2\mathcal{A}^{\mathrm{ph}}}. \tag{4}$$

Following Carcione (2007), Červený and Pšenčík (2008) derive the following expression for the "group" quality factor:

$$Q^{\mathrm{gr}} = \frac{\mathbf{p}^R \cdot \mathbf{F}^R}{2\mathbf{p}^I \cdot \mathbf{F}^R}, \tag{5}$$

where $\mathbf{F}^R$ denotes the real part of the Poynting vector. The real part of the complex-valued Poynting vector is parallel to the group-velocity vector. The time-averaged energy flux is given by

$$F_i^R = \kappa\,\mathrm{Re}[\tilde{a}_{ijkl}\tilde{p}_l\,\tilde{g}_j^*\,\tilde{g}_k], \tag{6}$$

where the asterisk denotes the complex conjugate, κ is a constant, and the components of the complex-valued polarization vector $\tilde{\mathbf{g}}$ are normalized using the condition $\tilde{\mathbf{g}}\cdot\tilde{\mathbf{g}} = 1$. Equation 5 involves a projection of the attenuation and propagation vectors onto the Poynting vector, so Q^{gr} quantifies the energy decay along the ray-path. Definitions similar to that in equation 5 have been used to introduce the group attenuation coefficient (e.g., Behura and Tsvankin, 2009). For weakly attenuative media, the quality factor Q^{gr} is independent of the inhomogeneity angle and coincides with the quality factor corresponding to the phase attenuation coefficient for $\xi = 0$ (Q^{ph}, see equation 4). This result was derived independently by Behura and Tsvankin (2009) and Červený and Pšenčík (2008, 2009). Behura and Tsvankin (2009) also show that the group attenuation coefficient remains practically independent of the inhomogeneity angle even for strong attenuation.

ASYMPTOTIC GREEN'S FUNCTION IN HOMOGENEOUS ATTENUATIVE ANISOTROPIC MEDIA

Here, we derive the asymptotic Green's function in the frequency domain for a homogeneous, attenuative, arbitrarily anisotropic medium. The analysis is valid for all three wave modes (P, S_1, and S_2), but it breaks down in the vicinity of S-wave singularities where the Christoffel equation has two equal or close eigenvalues. According to the causality principle, the stiffnesses in attenuative media should be, in general, frequency-dependent (Aki and Richards, 1980). Although we do not explicitly account for velocity dispersion, the following analysis is valid for a frequency-dependent stiffness tensor.

The exact Green's function for each mode can be found as the solution of the viscoelastic wave equation (Appendix A, equation A-9):

$$G_{kn}(\mathbf{x},\mathbf{x}^0,\omega) = \frac{i\omega}{(2\pi)^2}\int_{-\infty}^{\infty}\int_{-\infty}^{\infty}\left[\frac{\tilde{S}_{kn}}{\partial[\det(\tilde{\mathbf{\Gamma}}-\mathbf{I})]/\partial p_3}\right]_{p_3=\tilde{p}_3^r} e^{\,\omega R\tilde{\phi}}\,\mathrm{d}p_1\mathrm{d}p_2, \tag{7}$$

where the x_3-axis points in the source-receiver direction and

$$\tilde{\phi} = i\tilde{p}_3^r. \tag{8}$$

Here, R is the source-receiver distance, p_j are the slowness components, $\tilde{\Gamma}_{ik} = \tilde{a}_{ijkl}p_jp_l$ is the Christoffel matrix, $\mathbf{I}$ is the identity matrix, $\tilde{S}_{kn}$ are the cofactors of the matrix $\tilde{\mathbf{\Gamma}}-\mathbf{I}$, and $\tilde{p}_3^r = \tilde{p}_3(p_1,p_2)$ is the solution of the complex-valued Christoffel equation $\det[\tilde{a}_{ijkl}p_jp_l - \delta_{ik}] = 0$ corresponding to the mode of interest.

If we assume that $\omega R/v \gg 1$ (v is the average of the group velocity over all angles), G_{kn} (equation 7) can be evaluated by iterative application of the steepest-descent method (Bleistein, 2012). The saddle-point condition satisfied at $[\tilde{p}_1^s, \tilde{p}_2^s]$ is

$$\frac{\partial\tilde{\phi}}{\partial p_1} = \frac{\partial\tilde{\phi}}{\partial p_2} = 0. \tag{9}$$

The iterative steepest-descent method yields:

$$G_{kn}(\mathbf{x},\mathbf{x}^0,\omega) = \frac{1}{2\pi R}\frac{1}{\sqrt{|\det\tilde{\mathbf{\Phi}}''|}}\frac{\tilde{S}_{kn}}{\partial[\det(\tilde{\mathbf{\Gamma}}-\mathbf{I})]/\partial p_3} \times \exp\left(i\omega R\tilde{p}_3^r - \frac{i}{2}\arg[\det\tilde{\mathbf{\Phi}}'']\right), \tag{10}$$

where $\tilde{\mathbf{\Phi}}''$ is the Hessian matrix of the second-order partial derivatives of $\tilde{\phi}$ with respect to p_1 and p_2; all quantities are obtained at the saddle point.

We now discuss the identification of the saddle point $[\tilde{p}_1^s, \tilde{p}_2^s]$. Equation 9 implies that

$$\left[\frac{\partial\tilde{p}_3(p_1,p_2)}{\partial p_1}\right]_{\tilde{p}_1^s,\tilde{p}_2^s} = 0 \tag{11}$$

and

$$\left[\frac{\partial\tilde{p}_3(p_1,p_2)}{\partial p_2}\right]_{\tilde{p}_1^s,\tilde{p}_2^s} = 0. \tag{12}$$

Each eigenvalue $\tilde{\lambda}^{(m)}$ of the Christoffel matrix $\tilde{\Gamma}_{ik} = \tilde{a}_{ijkl}p_jp_l$ is a function of the slowness vector (with $\tilde{p}_3 = \tilde{p}_3^r$) (see Appendix B, equation B-9):

$$\tilde{\lambda}^{(m)} = \lambda(\tilde{a}_{ijkl},\tilde{p}_j) = \tilde{a}_{ijkl}\tilde{p}_j\,\tilde{p}_l\,\tilde{g}_i^{(m)}\tilde{g}_k^{(m)}, \tag{13}$$

where m takes values from 1 to 3 and $\tilde{\mathbf{g}}^{(m)}$ denotes the corresponding unit polarization vector introduced in Appendix B. The largest eigenvalue $\tilde{\lambda}^{(1)} = 1$ is obtained for the slowness vector of the fastest mode (P-wave). The partial derivatives in equations 11 and 12 can be calculated from the function $\lambda(\tilde{a}_{ijkl}, \tilde{p}_j)$ (equation 13) using the analytic implicit function theorem (Krantz and Parks, 2002):

$$\left[\frac{\partial \tilde{p}_3(p_1, p_2)}{\partial p_1}\right]_{\tilde{p}_1^s, \tilde{p}_2^s} = -\left[\frac{\partial\lambda/\partial p_1}{\partial\lambda/\partial p_3}\right]_{\tilde{p}_1^s, \tilde{p}_2^s} \tag{14}$$

and

$$\left[\frac{\partial \tilde{p}_3(p_1, p_2)}{\partial p_2}\right]_{\tilde{p}_1^s, \tilde{p}_2^s} = -\left[\frac{\partial\lambda/\partial p_2}{\partial\lambda/\partial p_3}\right]_{\tilde{p}_1^s, \tilde{p}_2^s}, \tag{15}$$

where $\partial\lambda/\partial p_j$ is given by equation B-10; $\partial\lambda/\partial p_3 \neq 0$ because the x_3-axis points in the source-receiver direction. Next, we introduce the energy-velocity vector $\tilde{\boldsymbol{\mathcal{U}}}$ (Vavryčuk, 2007) as

$$\tilde{\mathcal{U}}_j = \frac{1}{2}\frac{\partial\lambda}{\partial p_j}. \tag{16}$$

Equations 14 and 15 imply that at the saddle point,

$$\tilde{\mathcal{U}}_1 = \tilde{\mathcal{U}}_2 = 0. \tag{17}$$

Hence, the real and imaginary parts of $\tilde{\boldsymbol{\mathcal{U}}}$ are parallel to the vector connecting the source and receiver (i.e., in our case to the x_3-axis). Note that Červený et al. (2008) arrived at the same conclusion for weakly dissipative media using perturbation analysis. Equations 16 and 17 can be used to constrain the slowness vector $\tilde{\mathbf{p}}$ that corresponds to the plane wave that makes the most significant contribution to the wavefield at the receiver location. It is convenient to parametrize $\tilde{\mathbf{p}}$ in the following way (Červený and Pšenčík, 2005):

$$\tilde{\mathbf{p}} = \tilde{\sigma}\,\mathbf{n} + i\,D\,\mathbf{m}, \tag{18}$$

where $\mathbf{n}$ is a unit vector in the phase direction, $\tilde{\sigma}$ is a complex-valued quantity that corresponds to the projection of the slowness vector onto the vector $\mathbf{n}$, $\mathbf{m}$ is chosen to be perpendicular to $\mathbf{n}$ (i.e., $\mathbf{n}\cdot\mathbf{m} = 0$), and D is called the *inhomogeneity parameter* (Červený and Pšenčík, 2005). For plane waves, $\tilde{\sigma}$ is found as one of the solutions of the Christoffel equation corresponding to a particular mode, whereas D can vary between zero and infinity. The parameters $\tilde{\sigma}$ and D are determined by the saddle-point condition for point-source radiation. Therefore, we use the condition in equation 17 to set up the following constrained optimization problem for $\tilde{\sigma}$ and D:

$$\text{Minimize } \tilde{\mathcal{U}}_1^2 + \tilde{\mathcal{U}}_2^2, \quad \text{subject to } \tilde{\lambda}^{(1)} = 1. \tag{19}$$

This problem is nonlinear, and the values of $\tilde{\sigma}$ and D at the global minimum yield the slowness vector at the saddle point.

Equation 10 can be simplified once the saddle point has been found. From equations 16, 17, and B-15, we have

$$\tilde{p}_3\tilde{\mathcal{U}}_3 = \tilde{\lambda}^{(1)} = 1. \tag{20}$$

The phase function at the saddle point (equation 8) can, therefore, be written as

$$\tilde{\phi} = i\tilde{p}_3^r = i\frac{1}{\tilde{\mathcal{U}}_3}. \tag{21}$$

In elastic media, equation 16 defines the components of the group-velocity vector. In attenuative media, the real and imaginary parts of $\tilde{\boldsymbol{\mathcal{U}}}$ determine the traveltime and energy dissipation, respectively. Using equations B-16 and 16, we have

$$\frac{\tilde{S}_{kn}}{\partial[\det(\tilde{\boldsymbol{\Gamma}} - \mathbf{I})]/\partial p_3} = \frac{\tilde{S}_{kn}}{\tilde{S}_{ij}(\partial\tilde{\Gamma}_{ij}/\partial p_3)} = \frac{\tilde{g}_k^{(1)}\tilde{g}_n^{(1)}}{2\tilde{\mathcal{U}}_3}. \tag{22}$$

Equation 10 can then be rewritten as

$$G_{kn}(\mathbf{x},\mathbf{x}^0,\omega) = \frac{\tilde{g}_k^{(1)}\tilde{g}_n^{(1)}}{4\pi R\tilde{\mathcal{U}}_3\sqrt{|\det\tilde{\boldsymbol{\Phi}}''|}}\exp\left(i\frac{\omega R}{\tilde{\mathcal{U}}_3} - \frac{i}{2}\arg[\det\tilde{\boldsymbol{\Phi}}'']\right), \tag{23}$$

where the components of the matrix $\tilde{\boldsymbol{\Phi}}''$ are computed at the saddle point using the implicit function theorem:

$$\tilde{\Phi}''_{MN} = -\left[\frac{\partial^2\lambda/(\partial p_M\partial p_N)}{\partial\lambda/\partial p_3}\right]_{\tilde{p}_1^s, \tilde{p}_2^s}; \tag{24}$$

the indices M and N take values from 1 to 2. The second-order partial derivatives of $\lambda(\tilde{a}_{ijkl}, \tilde{p}_j)$ can be evaluated using equation B-11.

Equation 23 was derived for a rotated coordinate frame with the x_3-axis pointing in the source-receiver direction. The Green's function in a general (global) Cartesian coordinate frame takes the following form:

$$G_{kn}(\mathbf{x},\mathbf{x}^0,\omega) = \frac{\tilde{g}_k^{(1)}\tilde{g}_n^{(1)}}{4\pi R|\tilde{\boldsymbol{\mathcal{U}}}|\sqrt{|\det\tilde{\boldsymbol{\Phi}}''|}} \times\exp\left(i\frac{\omega R}{|\tilde{\boldsymbol{\mathcal{U}}}|} - \frac{i}{2}\arg[\det\tilde{\boldsymbol{\Phi}}'']\right), \tag{25}$$

where $\tilde{\boldsymbol{\mathcal{U}}}$ is the energy-velocity vector in the source-receiver direction and $|\tilde{\boldsymbol{\mathcal{U}}}|$ denotes its complex-valued magnitude ($|\tilde{\boldsymbol{\mathcal{U}}}| = \tilde{\mathcal{U}}_3$ from equation 16.

For TI media, equation 25 reduces to the expression for the Green's function derived by Zhu (2006). Although the asymptotic analysis carried out above is similar to that presented by Vavryčuk (2007), we proved (rather than assumed) that at the saddle point, the real and imaginary parts of the energy-velocity vector are parallel to each other.

RAY-PERTURBATION ANALYSIS FOR ANISOTROPIC ATTENUATIVE MEDIA

Here, we briefly review the ray-tracing methodology of Červený and Pšenčík (2009), which is applicable in weakly attenuative, anisotropic, heterogeneous media with smooth spatial variations of the stiffness tensor. We provide expressions for the ray-theoretical Green's function and analyze the orientation of the slowness vector in homogeneous attenuative models. These results will be compared to those obtained in the previous section.

Following Klimeš (2002), Červený and Pšenčík (2009) treat the traveltime as a complex-valued quantity, with the real part

contributing to the phase (arrival time) and the imaginary part to the dissipation along the ray. The traveltime and its spatial gradients are computed as perturbations of the corresponding real-valued quantities obtained along the ray traced in the reference elastic medium. In the density-normalized stiffness tensor given by equation 1, the real part a^R_{ijkl} is treated here as corresponding to the reference elastic medium, and the imaginary part a^I_{ijkl} is the attenuation-related perturbation.

We consider the linear perturbation Hamiltonian $\mathcal{H}(\alpha)$ defined in Červený and Pšenčík (2009):

$$\mathcal{H}(\alpha) = \mathcal{H}^0 + \alpha \triangle\mathcal{H}, \tag{26}$$

with

$$\triangle\mathcal{H} = \tilde{\mathcal{H}} - \mathcal{H}^0, \tag{27}$$

where $\mathcal{H}^0$ and $\tilde{\mathcal{H}}$ are the Hamiltonians corresponding to the (elastic) reference and (viscoelastic) perturbed medium, respectively. The perturbation parameter is denoted by α; $\alpha = 0$ corresponds to the reference elastic medium and $\alpha = 1$ to the perturbed attenuative medium. The reference Hamiltonian $\mathcal{H}^0$ can be expressed through the real-valued slowness ($\mathbf{p}^0$) and polarization ($\mathbf{g}^0$) vectors computed for the reference model:

$$\mathcal{H}^0 = \frac{1}{N}[a^R_{ijkl} p^0_j p^0_l g^0_i g^0_k]^{N/2}, \tag{28}$$

where N (integer) is the degree of the Hamiltonian. The perturbed Hamiltonian $\tilde{\mathcal{H}}$ is given by

$$\tilde{\mathcal{H}} = \frac{1}{N}[\tilde{a}_{ijkl} p^0_j p^0_l \tilde{g}_i \tilde{g}_k]^{N/2}, \tag{29}$$

where the complex polarization vector $\tilde{\mathbf{g}}$ is computed from the complex Christoffel matrix $\tilde{\Gamma}_{ik} = \tilde{a}_{ijkl} p^0_j p^0_l$ using equation B-8.

The traveltime and its spatial gradients can be expanded into a perturbation series in terms of the parameter α:

$$\tau(\alpha) \approx \tau^0 + \alpha \frac{\partial\tau}{\partial\alpha} + \cdots \tag{30}$$

and

$$\frac{\partial\tau}{\partial x_i} \approx \frac{\partial\tau^0}{\partial x_i} + \alpha \left[\frac{\partial^2\tau}{\partial x_i\, \partial\alpha}\right]_{\alpha=0} + \cdots, \tag{31}$$

where all terms correspond to the reference medium. The second-order partial derivatives in equation 31 can be computed using dynamic ray tracing (Červený and Pšenčík, 2009). The first-order approximation for the traveltime and the traveltime gradients in attenuative media can be obtained by substituting $\alpha = 1$ and retaining the first two terms of the expansion in equations 30 and 31. The real part of the traveltime contributes to the phase (i.e., the arrival time of the wave) and the imaginary part is responsible for the amplitude decay along the ray. The real part of the traveltime gradient corresponds to p^R and the imaginary part to p^I:

$$p^R_i = \mathrm{Re}\left[\frac{\partial\tau}{\partial x_i}\right] \approx p^0_i + \mathrm{Re}\left[\frac{\partial^2\tau}{\partial x_i\, \partial\alpha}\right]_{\alpha=0} \tag{32}$$

and

$$p^I_i = \mathrm{Im}\left[\frac{\partial\tau}{\partial x_i}\right] \approx \mathrm{Im}\left[\frac{\partial^2\tau}{\partial x_i\, \partial\alpha}\right]_{\alpha=0}. \tag{33}$$

The inhomogeneity angle can be computed from

$$\cos\,\xi = \frac{\mathbf{p}^I \cdot \mathbf{p}^R}{|\mathbf{p}^I||\mathbf{p}^R|}. \tag{34}$$

An approximate ray-theoretical Green's function in homogeneous, weakly attenuative media can be found by substituting the complex-valued traveltime into the expression for the reference elastic model (Gajewski and Pšenčík, 1992):

$$G_{kn}(\mathbf{x}, \mathbf{x}^0, \omega) = \frac{g_k\, g_n}{4\pi R\, |\boldsymbol{\mathcal{U}}| \sqrt{|K|}} \exp\left(i\omega\, \mathrm{Re}[\tilde{\tau}] + i\frac{\pi}{2} k_s\right) \times \exp(-\omega\, \mathrm{Im}[\tilde{\tau}]), \tag{35}$$

where $\mathbf{g}$ is the polarization vector, R is the source-receiver distance, $|\boldsymbol{\mathcal{U}}|$ is the magnitude of group velocity, K is the Gaussian curvature of the slowness surface, and k_s quantifies the phase shift due to K. Except for the complex traveltime $\tilde{\tau}$, all quantities are computed for the reference elastic medium.

The group quality factor responsible for energy decay along the ray and corresponding to the linear perturbation Hamiltonian (equation 26) can be found from

$$(Q^{\mathrm{gr}})^{-1} = -2\, \mathrm{Im}\, \tilde{\mathcal{H}}, \tag{36}$$

where $\tilde{\mathcal{H}}$ is defined in equation 29. Červený and Pšenčík (2009) also provide an approximation for the group-velocity components $\tilde{\mathcal{U}}_i$ in attenuative media:

$$\tilde{\mathcal{U}}_i = \left(1 - i\frac{1}{2Q^{\mathrm{gr}}}\right)\mathcal{U}_i, \tag{37}$$

where $\mathcal{U}_i$ is computed in the reference elastic medium. Hence, in homogeneous, weakly attenuative media, $\tilde{\tau} \approx R/|\tilde{\mathcal{U}}|$, and equation 35 can be rewritten as

$$G_{kn}(\mathbf{x}, \mathbf{x}^0, \omega) = \frac{g_k\, g_n}{4\pi R\, |\boldsymbol{\mathcal{U}}| \sqrt{|K|}} \exp\left(i\omega \frac{R}{|\tilde{\boldsymbol{\mathcal{U}}}|} + i\frac{\pi}{2} k_s\right). \tag{38}$$

Note that the complex-valued group velocity obtained from the perturbation analysis appears only in the exponential function, whereas the polarization vector and the Gaussian curvature K of the slowness surface, which control the magnitude of the Green's function, are computed for the reference elastic medium.

NUMERICAL EXAMPLES

In this section, the analytic results presented above are used to study the Green's function and the behavior of the slowness vector

in homogeneous, attenuative VTI media. Table 1 shows the parameters of the velocity and attenuation functions for four VTI models similar to those in Zhu (2006).

First, we compare the P-wave group attenuation coefficients obtained from the asymptotic analysis discussed above and perturbation theory. The asymptotic coefficient is computed from equation 5 with the slowness $\tilde{\mathbf{p}}$ and the corresponding Poynting vector $\mathbf{F}$ obtained from the asymptotic analysis. Equation 36 is used to find the attenuation coefficient from perturbation analysis with the Hamiltonians of degrees $N = -1$ and 2.

The example in Figure 1 shows that the group quality factor Q^{gr} (equation 5) obtained from the perturbation theory is close to the asymptotic value; also, the quality factors for the two choices of N coincide. Although the attenuation-anisotropy coefficients ϵ_Q and δ_Q for models 3 and 4 are equal to zero, there is a slight angular variation in Q^{gr} for model 3; this is due to the combined effect of velocity anisotropy and the difference between the values of Q_{P0} and Q_{S0} (Zhu and Tsvankin, 2006).

Substituting the slowness vector computed from the asymptotic analysis into the Christoffel matrix and using equation B-8 yields the plane-wave polarization vector that corresponds to the saddle-point condition. Similarly, substituting the slowness vector obtained by ray tracing in the reference medium into the Christoffel matrix yields the polarization vector in the perturbation analysis. We found that the asymptotic and perturbation approaches produce the polarization vectors with close magnitudes.

Figure 2 displays the phase of the vertical component of the polarization vector $\tilde{g}_3$ (arg $\tilde{g}_3$) computed from the asymptotic and perturbation methods for models 1–4. The function arg $\tilde{g}_3$ monotonically increases with the group angle ϕ for models 1–3, whereas it is negligible for model 4 because the attenuation function is isotropic. Note that the magnitude of $\tilde{g}_3$ for angles approaching 90° (near the isotropy plane) is small, which distorts the phase of $\tilde{g}_3$. For all models, the asymptotic and perturbation methods yield similar values of arg $\tilde{g}_3$, with some deviations only for large angles ϕ.

Next, we analyze the component G_{33} of the Green's function obtained from asymptotic analysis (equation 23):

$$G_{33}(\mathbf{x},\mathbf{x}^0,\omega) = \frac{\tilde{g}_3^{(1)}\tilde{g}_3^{(1)}}{4\pi R|\tilde{\boldsymbol{\mathcal{U}}}|\sqrt{|\det\tilde{\boldsymbol{\Phi}}''|}} \times \exp\left(i\frac{\omega R}{|\tilde{\boldsymbol{\mathcal{U}}}|} - \frac{i}{2}\arg[\det\tilde{\boldsymbol{\Phi}}'']\right). \quad (39)$$

The same component produced by the perturbation approach has the form (equation 38):

$$G_{33}(\mathbf{x},\mathbf{x}^0,\omega) = \frac{g_3^{(1)}g_3^{(1)}}{4\pi R|\boldsymbol{\mathcal{U}}|\sqrt{|K|}} \times \exp\left(i\omega\frac{R}{|\tilde{\boldsymbol{\mathcal{U}}}|} + i\frac{\pi}{2}k_s\right). \quad (40)$$

The polarization vector, group velocity, and Hessian of the slowness surface in equation 39 are complex-valued. The only complex-valued quantity in equation 40 is the perturbed group-velocity vector $\tilde{\boldsymbol{\mathcal{U}}}$, which determines the attenuation along the ray. Our tests show that the magnitude and argument of the energy-velocity vector $\tilde{\boldsymbol{\mathcal{U}}}$ computed from the asymptotic analysis (equation 16) are close to those computed from perturbation analysis (equation 37). Also, the difference between the magnitudes of the Hessian of the slowness surface (det $\tilde{\boldsymbol{\Phi}}''$) in equation 39 and of the Gaussian curvature K in equation 40 is small.

Although the magnitudes of the complex-valued quantities (the polarization vector, group velocity, and the Hessian of the slowness

Table 1. Homogeneous TI models with anisotropic velocity and attenuation functions. The parameters V_{P0} and V_{S0} are the P- and S-wave symmetry-direction velocities, Q_{P0} and Q_{S0} are the P-wave and S-wave symmetry-direction quality factors, and ϵ_Q and δ_Q are the attenuation-anisotropy parameters defined in Zhu and Tsvankin (2006) and Tsvankin and Grechka (2011).

Model	1	2	3	4
V_{P0} (km/s)	3.00	3.00	3.00	3.00
V_{S0} (km/s)	1.50	1.50	1.50	1.50
ϵ	0.10	0.40	0.40	0.40
δ	0.05	0.25	0.25	0.25
Q_{P0}	10	10	100	10
Q_{S0}	6	6	10	10
ϵ_Q	−0.20	−0.45	0	0
δ_Q	−0.10	−0.50	0	0

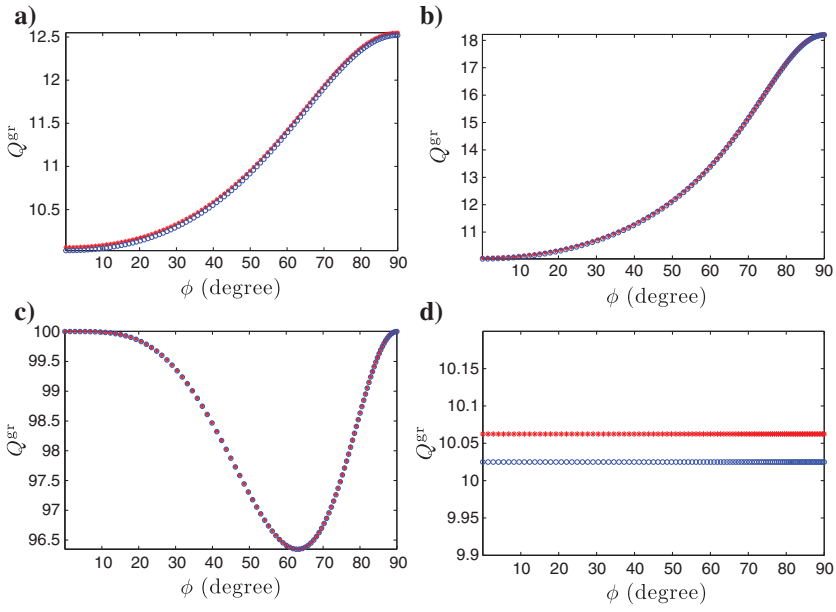

Figure 1. Comparison of the P-wave group quality factors (equation 5) as a function of the group angle ϕ with the vertical obtained from the asymptotic (blue circles) and perturbation (red stars) analysis for (a) model 1, (b) model 2, (c) model 3, and (d) model 4. The models are defined in Table 1.

surface) in equation 39 are close to their real-valued counterparts in equation 40, the phase of these quantities influence the phase of the Green's function.

The attenuation-induced phase distortion ϕ_d of the component G_{33} in equation 39 can be expressed as

$$\phi_d = 2\ \arg[\tilde{g}_3^{(1)}] - \frac{1}{2}\arg[\det\ \tilde{\mathbf{\Phi}}''] - \arg[|\tilde{\boldsymbol{\mathcal{U}}}|]. \qquad (41)$$

The values of ϕ_d for the models in Table 1 range between $-5°$ and $5°$, and hence do not significantly distort the phase of the Green's function (Figure 3). The other components of the Green's function exhibit properties similar to those of G_{33}.

Figure 4 compares the inhomogeneity angle ξ computed from the perturbation approach (equation 34) and the asymptotic analysis. The values of ξ obtained by the two methods are close to one another for models 1 and 3. There is a discrepancy for model 2, which can be expected because P-wave attenuation for that model is strongly anisotropic. Although both methods used here are approximate, the asymptotic analysis is expected to be more accurate for models with strong attenuation and pronounced attenuation anisotropy. Although model 4 has substantial attenuation and an anisotropic velocity function, the inhomogeneity angle for that

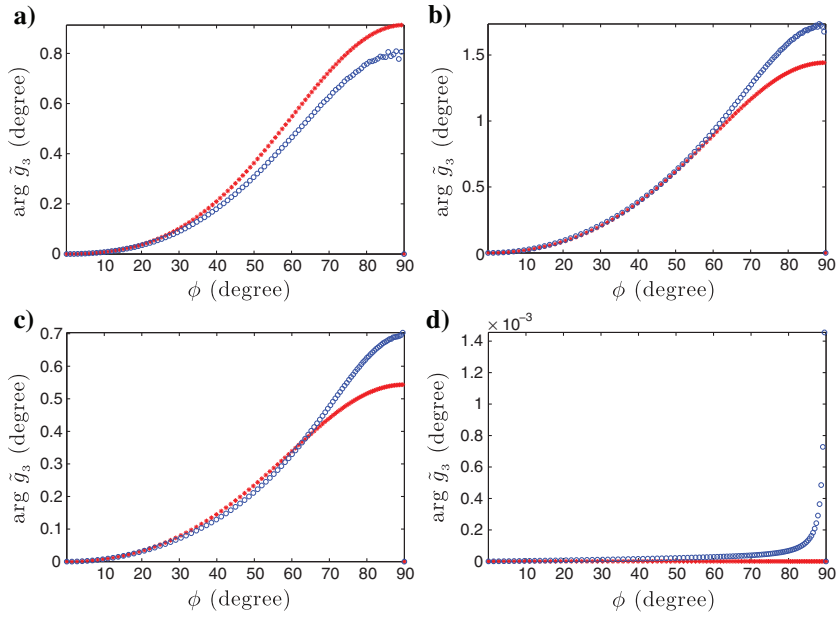

Figure 2. Phase of the vertical component $\tilde{g}_3$ of the polarization vector computed from the asymptotic (blue circles) and perturbation (red stars) analysis for (a) model 1, (b) model 2, (c) model 3, and (d) model 4.

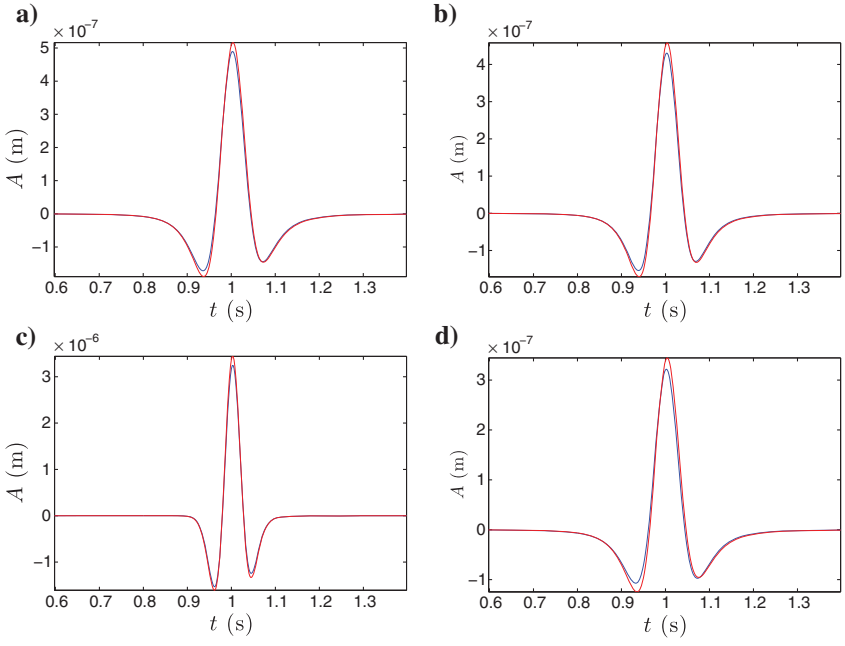

Figure 3. Asymptotic (blue) and perturbation (red) component G_{33} of the Green's function convolved with a Ricker wavelet of peak frequency 10 Hz for (a) model 1, (b) model 2, (c) model 3, and (d) model 4. The source-receiver line makes an angle of 45° with the symmetry axis, and the propagation time is 1 s.

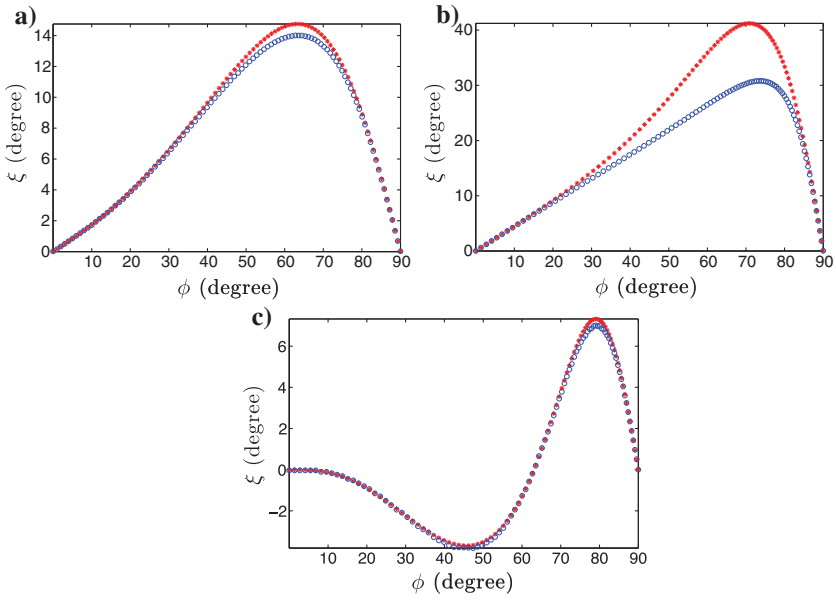

Figure 4. P-wave inhomogeneity angle computed from the asymptotic (blue circles) and perturbation (red stars) analysis for (a) model 1, (b) model 2, and (c) model 3.

model vanishes because the components Q_{ij} of the phase quality factor (defined in Zhu and Tsvankin, 2006) are identical (see Appendix C).

CONCLUSIONS

We presented a rigorous derivation of the asymptotic Green's function in homogeneous, attenuative, arbitrarily anisotropic media using the steepest-descent method. Application of the saddle-point condition helps identify the plane wave that makes the most significant contribution to the displacement field of each mode. Our results make it possible to evaluate the inhomogeneity angle and describe the complex-valued group-velocity vector in the high-frequency (far-field) approximation.

P-wave signatures obtained from our asymptotic analysis for TI media were compared with the same quantities computed by ray-perturbation theory. The asymptotic energy-velocity vector that describes the traveltime and attenuation along the ray is close to the perturbed group-velocity vector. The inhomogeneity angles computed from the saddle-point condition and perturbation theory differ only for strongly attenuative models. Although complex-valued quantities change the phase of the Green's function in attenuative media, the magnitude of the phase distortion is small even for models with strong attenuation anisotropy.

ACKNOWLEDGMENTS

We are grateful to the members of the A(nisotropy)-Team of the Center for Wave Phenomena (CWP), Colorado School of Mines, for fruitful discussions. The authors would like to thank I. Pšenčík for stimulating discussions and his rigorous critique. C. Thomson (Schlumberger), P. Martin (CSM), and M. Reynolds (CU Boulder) provided valuable help with asymptotic analysis and linear algebra. We are grateful to the three anonymous reviewers for their constructive suggestions. This work was supported by the Consortium Project on Seismic Inverse Methods for Complex Structures at CWP.

APPENDIX A

EXACT GREEN'S FUNCTION FOR ATTENUATIVE ANISOTROPIC MEDIA

The viscoelastic wave equation in the frequency-wavenumber domain for a homogeneous, attenuative, anisotropic medium can be written as (Zhu, 2006; Carcione, 2007)

$$(\tilde{a}_{ijkl}\,k_j k_l - \omega^2\delta_{ik})\tilde{U}_k(\mathbf{k},\omega) = \tilde{f}_i(\mathbf{k},\omega), \tag{A-1}$$

where ω is the frequency, $\tilde{a}_{ijkl}$ are the components of the density-normalized stiffness tensor, k_j are the wavenumbers, $\tilde{\mathbf{U}}$ is the displacement vector, and $\tilde{f}(\mathbf{k},\omega)$ is the body force per unit volume (source term). Summation over repeated indices (changing from 1 to 3) is implied.

The frequency-domain displacement can be found as the triple Fourier integral:

$$\tilde{u}_k(\mathbf{x},\omega) = \frac{1}{(2\pi)^3}\int_{-\infty}^{\infty}\tilde{U}_k(k,\omega)e^{ik_j x_j}\,\mathrm{d}\mathbf{k}, \tag{A-2}$$

where $\mathrm{d}\mathbf{k} = \mathrm{d}k_1\mathrm{d}k_2\mathrm{d}k_3$ and

$$\tilde{U}_k(k,\omega) = \frac{\tilde{B}_{ki}\,\tilde{f}_i(k_j,\omega)}{\det\tilde{\mathbf{D}}}. \tag{A-3}$$

The matrix $\tilde{\mathbf{D}}$ ($\tilde{D}_{ki} = \tilde{a}_{ijkl}\,k_j\,k_l - \omega^2\delta_{ik}$) with cofactors $\tilde{B}_{ki}$ is closely related to the Christoffel matrix. The source in equation A-1 can be defined as a point impulsive force applied at location $\mathbf{x}_0$ parallel to the x_n-axis:

$$\tilde{f}_i(\mathbf{k},\,\omega) = \delta_{in}e^{-ik_j x_j^0}. \tag{A-4}$$

The particle displacement from this source is the Green's function G_{kn}:

$$G_{kn}(\mathbf{x},\mathbf{x}^0,\omega) = \frac{1}{(2\pi)^3}\int_{-\infty}^{\infty}\frac{\tilde{B}_{ki}\delta_{in}}{\det\tilde{\mathbf{D}}}e^{ik_j(x_j-x_j^0)}\,\mathrm{d}\mathbf{k}. \tag{A-5}$$

Following Červený (2001), we rotate the coordinate frame to align the x_3-axis with the source-receiver direction. Equation A-5 in the rotated coordinate frame now reads

$$G_{kn}(\mathbf{x},\mathbf{x}^0,\omega) = \frac{1}{(2\pi)^3}\int_{-\infty}^{\infty}\frac{\tilde{B}_{ki}\,\delta_{in}}{\det\tilde{\mathbf{D}}}e^{ik_3 R}\,\mathrm{d}\mathbf{k}, \tag{A-6}$$

where $R = \sqrt{(x_1-x_1^0)^2 + (x_2-x_2^0)^2 + (x_3-x_3^0)^2}$ is the source-receiver distance. The Bond transformation has to be applied to the stiffness tensor to account for the coordinate rotation. Note that

the components of the wave vector k_j also correspond to the rotated coordinate frame. For convenience, here we retain the symbols introduced in the previous equations, which were defined in the unrotated coordinates.

The integral over k_3 in equation A-6 can be extended into the complex plane by representing the vertical wavenumber as $\tilde{k}_3 = \mathrm{Re}\, k_3 + i\, \mathrm{Im}\, k_3$. The closed contour includes the real axis and a semicircle with an infinitely large radius in the upper half-plane (because $R > 0$). The integral can then be evaluated by the residue theorem (i.e., by computing the residues at the poles), as described by Aki and Richards (1980), Tsvankin and Chesnokov (1990), and Tsvankin (1995). The poles correspond to the roots of the Christoffel equation for k_3:

$$\det \tilde{\mathbf{D}} = \det[\tilde{a}_{ijkl}\, k_j\, k_l - \omega^2\, \delta_{ik}] = 0. \tag{A-7}$$

Equation A-7 is a sixth-order polynomial in k_3 with complex coefficients that can have at most six distinct roots corresponding to the up- and downgoing P-, S_1-, and S_2-waves.

For homogeneous (nondecaying) waves in unbounded nonattenuative media, the roots of k_3 lie on the real k_3-axis. Then, the integral i n equation A-6 can be evaluated by introducing small attenuation, moving the roots to the complex plane, and applying the residue theorem (Tsvankin, 1995). Alternatively, the integral over k_3 can be evaluated using Cauchy's principal value (Bleistein, 1984).

In the presence of attenuation, the roots of equation A-7 lie away from the real axis. The pole $\tilde{k}_3^r = \tilde{k}_3(k_1, k_2)$, which corresponds to a certain mode (e.g., P-waves) and is located inside the integration contour, yields the residue for that mode. Hence, the integral over k_3 in equation A-6 can be evaluated using the residue at the pole, and the Green's function is expressed as the following double integral:

$$G_{kn}(\mathbf{x}, \mathbf{x}^0, \omega) = \frac{i}{(2\pi)^2} \int_{-\infty}^{\infty} \int_{-\infty}^{\infty} \left[\frac{\tilde{B}_{kn}}{\partial(\det \tilde{\mathbf{D}})/\partial k_3} \right]_{k_3 = \tilde{k}_3^r} e^{i \tilde{k}_3^r R \hat{x}_3}\, \mathrm{d}k_1\, \mathrm{d}k_2. \tag{A-8}$$

Substituting $k_j = \omega p_j$, where p_j denotes the components of the slowness vector, yields $\det \tilde{\mathbf{D}} = \omega^6 \det(\tilde{\Gamma}_{ik} - \delta_{ik})$, where $\tilde{\Gamma}_{ik} = \tilde{a}_{ijkl}\, p_j\, p_l$. The cofactors of $\tilde{\mathbf{\Gamma}} - \mathbf{I}$ ($\mathbf{I}$ is the identity matrix) are denoted by $\tilde{S}_{kn}$ and $\tilde{B}_{kn} = \omega^4 \tilde{S}_{kn}$. Equation A-8 can then be written as

$$G_{kn}(\mathbf{x}, \mathbf{x}^0, \omega) = \frac{i\,\omega}{(2\pi)^2} \int_{-\infty}^{\infty} \int_{-\infty}^{\infty} \left[\frac{\tilde{S}_{kn}}{\partial[\det(\tilde{\mathbf{\Gamma}} - \mathbf{I})]/\partial p_3} \right]_{p_3 = \tilde{p}_3^r} e^{i\omega R\, \tilde{p}_3^r}\, \mathrm{d}p_1\, \mathrm{d}p_2. \tag{A-9}$$

APPENDIX B

PROPERTIES OF THE CHRISTOFFEL MATRIX IN ATTENUATIVE ANISOTROPIC MEDIA

Here, we summarize the properties of the eigenvalues and eigenvectors of the Christoffel matrix in attenuative anisotropic media. These properties are used in the asymptotic and perturbation analyses presented in the main text. The results in this appendix are based on section 4.4 of Horn and Johnson (1990), which discusses complex symmetric matrices.

The components of the Christoffel matrix $\tilde{\mathbf{\Gamma}}$ in attenuative media are given by (see the main text)

$$\tilde{\Gamma}_{ik} = \tilde{a}_{ijkl}\, \tilde{p}_j \tilde{p}_l, \tag{B-1}$$

where $\tilde{a}_{ijkl}$ is the density-normalized complex stiffness tensor and $\tilde{\mathbf{p}}$ is the complex-valued slowness vector.

The eigenvector-eigenvalue problem for matrix $\tilde{\mathbf{\Gamma}}$ can be written as

$$\tilde{\mathbf{\Gamma}}\, \tilde{\mathbf{V}} = \tilde{\mathbf{V}}\, \tilde{\mathbf{\Lambda}}, \tag{B-2}$$

where $\tilde{\mathbf{\Lambda}}$ is the diagonal matrix of the eigenvalues, and the columns of $\tilde{\mathbf{V}}$ contain the corresponding eigenvectors. The matrix $\tilde{\mathbf{V}}$ is nonsingular (Horn and Johnson, 1990), so

$$\tilde{\mathbf{\Gamma}} = \tilde{\mathbf{V}}\, \tilde{\mathbf{\Lambda}}\, \tilde{\mathbf{V}}^{-1} \tag{B-3}$$

and

$$\tilde{\mathbf{\Lambda}} = \tilde{\mathbf{V}}^{-1} \tilde{\mathbf{\Gamma}}\, \tilde{\mathbf{V}}\,. \tag{B-4}$$

If the eigenvalues of the Christoffel matrix are distinct, the matrix $\tilde{\mathbf{V}}$ satisfies

$$\tilde{\mathbf{V}}^{\mathrm{T}}\, \tilde{\mathbf{V}} = \tilde{\mathbf{D}}, \tag{B-5}$$

where $\tilde{\mathbf{D}}$ is a diagonal matrix. The Christoffel matrix can be diagonalized in the following way:

$$\tilde{\mathbf{\Gamma}} = \tilde{\mathbf{G}}\, \tilde{\mathbf{\Lambda}}\, \tilde{\mathbf{G}}^{\mathrm{T}}, \tag{B-6}$$

and

$$\tilde{\mathbf{\Lambda}} = \tilde{\mathbf{G}}^{\mathrm{T}} \tilde{\mathbf{\Gamma}}\, \tilde{\mathbf{G}}\,, \tag{B-7}$$

with

$$\tilde{\mathbf{G}} = \tilde{\mathbf{V}}\, \tilde{\mathbf{D}}^{-1/2}. \tag{B-8}$$

The matrix $\tilde{\mathbf{G}}$ is complex orthonormal; i.e., $\tilde{\mathbf{G}}^{\mathrm{T}} \tilde{\mathbf{G}} = \tilde{\mathbf{G}}\, \tilde{\mathbf{G}}^{\mathrm{T}} = \mathbf{I}$.

In purely elastic media $\tilde{\mathbf{D}} = \mathbf{I}$, and consequently $\tilde{\mathbf{V}}^{\mathrm{T}} = \tilde{\mathbf{V}}^{-1}$ and $\tilde{\mathbf{V}} = \tilde{\mathbf{G}}$. The eigenvector matrix $\tilde{\mathbf{V}}$ then includes the polarization vectors of the three wave modes. Choosing the columns of $\tilde{\mathbf{G}}$ as the polarization vectors helps extend expressions derived for elastic media to attenuative models.

Next, we provide expressions for quantities related to the complex Christoffel matrix used throughout this paper. The results below are based on sections 3.6.2 and 4.14.1 of Červený (2001), with the real-valued stiffness coefficients and slowness vector replaced by the corresponding complex-valued quantities. We denote the eigenvalues (elements of $\tilde{\mathbf{\Lambda}}$) by $\tilde{\lambda}^{(1)}$, $\tilde{\lambda}^{(2)}$, and $\tilde{\lambda}^{(3)}$, and the corresponding polarization vectors (columns of $\tilde{\mathbf{G}}$) by $\tilde{\mathbf{g}}^{(1)}$, $\tilde{\mathbf{g}}^{(2)}$, and $\tilde{\mathbf{g}}^{(3)}$. Using equation B-7, the eigenvalue $\tilde{\lambda}^{(1)}$ can be found as

$$\lambda^{(1)} = \tilde{g}_i^{(1)} \tilde{a}_{ijkl}\ \tilde{p}_j\, \tilde{p}_l\ \tilde{g}_k^{(1)}. \tag{B-9}$$

Then, the derivatives $\partial\tilde{\lambda}^{(1)}/\partial\tilde{p}_n$ and $\partial^2\tilde{\lambda}^{(1)}/\left(\partial\tilde{p}_n\,\partial\tilde{p}_q\right)$ take the form:

$$\frac{\partial\tilde{\lambda}^{(1)}}{\partial\tilde{p}_n} = \frac{\partial\tilde{\Gamma}_{ik}}{\partial\tilde{p}_n}\ \tilde{g}_i^{(1)}\ \tilde{g}_k^{(1)}, \tag{B-10}$$

$$\frac{\partial^2\tilde{\lambda}^{(1)}}{\partial\tilde{p}_n\,\partial\tilde{p}_q} = \frac{\partial^2\tilde{\Gamma}_{ik}}{\partial\tilde{p}_n\,\partial\tilde{p}_q}\ \tilde{g}_i^{(1)}\ \tilde{g}_k^{(1)} + 2\frac{\partial\tilde{\Gamma}_{ik}}{\partial\tilde{p}_n}\ \tilde{g}_i^{(1)}\frac{\partial\tilde{g}_k^{(1)}}{\partial\tilde{p}_q}, \tag{B-11}$$

$$\frac{\partial\tilde{\Gamma}_{ik}}{\partial\tilde{p}_n} = (\tilde{a}_{inqk} + \tilde{a}_{iqkn})\tilde{p}_q, \tag{B-12}$$

$$\frac{\partial^2\tilde{\Gamma}_{ik}}{\partial\tilde{p}_n\,\partial\tilde{p}_q} = \tilde{a}_{inqk} + \tilde{a}_{iqkn}, \tag{B-13}$$

and

$$\frac{\partial\tilde{g}_k^{(1)}}{\partial\tilde{p}_q} = \left[\frac{1}{\tilde{\lambda}^{(1)} - \tilde{\lambda}^{(2)}}\ \frac{\partial\Gamma_{in}}{\partial\tilde{p}_q}\ \tilde{g}_i^{(2)}\tilde{g}_n^{(1)}\right]\tilde{g}_k^{(2)} + \left[\frac{1}{\tilde{\lambda}^{(1)} - \tilde{\lambda}^{(3)}}\ \frac{\partial\tilde{\Gamma}_{in}}{\partial\tilde{p}_q}\ \tilde{g}_i^{(3)}\tilde{g}_n^{(1)}\right]\tilde{g}_k^{(3)}. \tag{B-14}$$

From equations B-9 and B-10, it follows that

$$\tilde{p}_n\frac{\partial\lambda^{(1)}}{\partial\tilde{p}_n} = 2\ \lambda^{(1)}. \tag{B-15}$$

Finally, the product $\tilde{g}_j^{(1)}\tilde{g}_k^{(1)}$ can be expressed as

$$\tilde{g}_j^{(1)}\tilde{g}_k^{(1)} = \frac{\tilde{S}_{jk}}{\mathrm{Tr}[\tilde{\mathbf{S}}]}, \tag{B-16}$$

where $\tilde{S}_{jk}$ represent the components of the cofactor matrix of $[\tilde{\mathbf{\Gamma}} - \tilde{\lambda}^{(1)}\mathbf{I}]$, and $\mathrm{Tr}[\tilde{\mathbf{S}}]$ is the trace of the cofactor matrix.

APPENDIX C

PERTURBATION ANALYSIS OF THE INHOMOGENEITY ANGLE

In this section, we present expressions for the propagation and attenuation vectors (and, hence, the inhomogeneity angle) in homogeneous, attenuative, anisotropic media using the method of perturbation Hamiltonians introduced by Červený and Pšenčík (2009). We also derive the conditions under which the inhomogeneity angle vanishes.

The second-order partial derivative in equation 31 can be evaluated using quadratures along the reference rays, as shown by Klimeš (2002) and Červený and Pšenčík (2009):

$$\frac{\partial^2\tau}{\partial x_i\,\partial\alpha} = \tilde{T}_k(\alpha)[Q_{ki}^{\mathrm{ray}}]^{-1}, \tag{C-1}$$

with the vector $\mathbf{T}(\alpha)$ given by

$$\tilde{T}_K(\alpha) = \tilde{T}_K^0(\alpha) + \tau\,\tilde{\mathcal{W}}_i P_{iK}^{\mathrm{ray}}, \quad K = 1, 2, \tag{C-2}$$

$$\tilde{\mathcal{W}}_i = \left(\frac{\partial\tilde{\mathcal{H}}}{\partial p_i} - \frac{\partial\mathcal{H}^0}{\partial p_i}\right), \tag{C-3}$$

and

$$\tilde{T}_3(\alpha) = \mathcal{H}^0 - \tilde{\mathcal{H}}. \tag{C-4}$$

The index K changes from 1 to 2, and the lowercase index k from 1 to 3. The real-valued matrices Q_{ik}^{ray} (not to be confused with the quality-factor matrix) and P_{ik}^{ray} are computed using dynamic ray tracing in the reference elastic medium:

$$Q_{ik}^{\mathrm{ray}} = \frac{\partial x_i}{\partial\gamma_k}, \quad P_{ik}^{\mathrm{ray}} = \frac{\partial p_i^0}{\partial\gamma_k}; \tag{C-5}$$

γ_k denotes a certain ray parameter (e.g., the initial phase angle or the traveltime along the ray). In equation C-2, the initial conditions $\tilde{T}_K^0(\alpha)$ are set to zero for a point source; for plane-wave propagation, $\tilde{T}_K^0(\alpha)$ may be chosen arbitrarily (Klimeš, 2002).

We now derive the conditions under which the inhomogeneity angle vanishes in homogeneous media. Substituting equations 28 and 29 into equation C-3 yields

$$\tilde{\mathcal{W}}_i = \tilde{a}_{ijkl}\,p_k\,\tilde{g}_j\,\tilde{g}_l - a_{ijkl}^R\,p_k\,g_j\,g_l. \tag{C-6}$$

For weakly dissipative media, we can use the approximation $\tilde{g} \approx g$ and reduce equation C-6 to

$$\tilde{\mathcal{W}}_i = -i\,a_{ijkl}^I\,p_k\,g_j\,g_l. \tag{C-7}$$

For the special case of identical components of the phase quality factor (i.e., $a_{ijkl}^I = a_{ijkl}^R/Q$), we have

$$\tilde{\mathcal{W}}_i = -i\,\frac{a_{ijkl}^R}{Q}\,p_k\,g_j\,g_l = -i\,\frac{\mathcal{U}_i}{Q}, \tag{C-8}$$

where $\mathcal{U}_i$ are the components of the group-velocity vector in the reference elastic medium. Substituting equation C-8 into equation C-2, we obtain

$$\tilde{T}_{K\alpha}(\gamma_3) = -i(\gamma_3 - \gamma_3^0)\frac{\mathcal{U}_i}{Q}P_{iK}^{\mathrm{ray}} = 0, \quad K = 1, 2 \tag{C-9}$$

because the group-velocity vector is orthogonal to the first two columns of the matrix $\mathbf{P}^{\mathrm{ray}}$ and $\mathcal{U}_i P_{iK} = 0$ (Červený, 2001). Equations 32 and 33 for p^R and p^I then take the form:

$$p_i^R = p_i^0 + \mathrm{Re}[\tilde{T}_{3\alpha}]\,p_i^0 \tag{C-10}$$

and

$$p_i^I = \mathrm{Im}[\tilde{T}_{3\alpha}]\, p_i^0, \tag{C-11}$$

where $p_i^0 = [Q_{3i}^{\mathrm{ray}}]^{-1}$ (Červený, 2001). From equations C-10 and C-11, it follows that p^R and p^I are parallel to p^0. Hence, the inhomogeneity angle vanishes in the case of identical Q_{ij} components, i.e., when the attenuation coefficients of all three modes are equal and isotropic. Note that the velocity function may still be angle-dependent (anisotropic). Furthermore, the inhomogeneity angle also vanishes for isotropic velocity and attenuation functions with different values of the quality factor for P- and S-waves. This can be proved by considering the expression for the Hamiltonian in isotropic media.

REFERENCES

Aki, K., and P. G. Richards, 1980, Quantitative seismology: Theory and methods, vol. 1: W.H. Freeman and Company.

Behura, J., and I. Tsvankin, 2009, Role of the inhomogeneity angle in anisotropic attenuation analysis: Geophysics, **74**, no. 5, WB177–WB191, doi: 10.1190/1.3148439.

Bleistein, N., 1984, Mathematical methods for wave phenomena: Academic Press.

Bleistein, N., 2012, Saddle point contribution for an *n*-fold complex-valued integral: Center for Wave Phenomena Research Report 741.

Borcherdt, R. D., 2009, Viscoelastic waves in layered media: Cambridge University Press.

Carcione, J., 2007, Wave fields in real media: Theory and numerical simulation of wave propagation in anisotropic, anelastic, porous and electromagnetic media: Elsevier.

Červený, V., 2001, Seismic ray theory: Cambridge University Press.

Červený, V., 2007, Reflection/transmission laws for slowness vectors in viscoelastic anisotropic media: Studia Geophysica et Geodaetica, **51**, 391–410, doi: 10.1007/s11200-007-0022-7.

Červený, V., L. Klimeš, and I. Pšenčík, 2008, Attenuation vector in heterogeneous, weakly dissipative, anisotropic media: Geophysical Journal International, **175**, 346–355, doi: 10.1111/j.1365-246X.2008.03850.x.

Červený, V., and I. Pšenčík, 2005, Plane waves in viscoelastic anisotropic media — I: Theory: Geophysical Journal International, **161**, 197–212, doi: 10.1111/j.1365-246X.2005.02589.x.

Červený, V., and I. Pšenčík, 2008, Quality factor *Q* in dissipative anisotropic media: Geophysics, **73**, no. 4, T63–T75, doi: 10.1190/1.2937173.

Červený, V., and I. Pšenčík, 2009, Perturbation Hamiltonians in heterogeneous anisotropic weakly dissipative media: Geophysical Journal International, **178**, 939–949, doi: 10.1111/j.1365-246X.2009.04218.x.

Gajewski, D., 1993, Radiation from point sources in general anisotropic media: Geophysical Journal International, **113**, 299–317, doi: 10.1111/j.1365-246X.1993.tb00889.x.

Gajewski, D., and I. Pšenčík, 1992, Vector wavefield for weakly attenuating anisotropic media by the ray method: Geophysics, **57**, 27–38, doi: 10.1190/1.1443186.

Hearn, D. J., and E. S. Krebes, 1990, On computing ray-synthetic seismograms for anelastic media using complex rays: Geophysics, **55**, 422–432, doi: 10.1190/1.1442851.

Horn, R. A., and C. R. Johnson, 1990, Matrix analysis: Cambridge University Press.

Klimeš, L., 2002, Second-order and higher-order perturbations of travel time in isotropic and anisotropic media: Studia Geophysica et Geodaetica, **46**, 213–248, doi: 10.1023/A:1019802003257.

Krantz, S. G., and H. R. Parks, 2002, The implicit function theorem: Springer.

Krebes, E. S., and L. H. T. Le, 1994, Inhomogeneous plane waves and cylindrical waves in anisotropic anelastic media: Journal of Geophysical Research, **99**, 899–919, doi: 10.1029/94JB02126.

Tsvankin, I., 1995, Seismic wavefields in layered isotropic media (course notes): Samizdat Press.

Tsvankin, I., and E. M. Chesnokov, 1990, Synthesis of body wave seismograms from point sources in anisotropic media: Journal of Geophysical Research, **95**, 11317–11331, doi: 10.1029/JB095iB07p11317.

Tsvankin, I., and V. Grechka, 2011, Seismology of azimuthally anisotropic media and seismic fracture characterization: SEG.

Vavryčuk, V., 2007, Asymptotic Green's function in homogeneous anisotropic viscoelastic media: Proceedings of the Royal Astronomical Society, **463**, 2689–2707, doi: 10.1098/rspa.2007.1862.

Wang, C. Y., and J. D. Achenbach, 1994, Elastodynamic fundamental solutions for anisotropic solids: Geophysical Journal International, **118**, 384–392, doi: 10.1111/j.1365-246X.1994.tb03970.x.

Zhu, Y., 2006, Seismic wave propagation in attenuative anisotropic media: Ph.D. thesis, Colorado School of Mines.

Zhu, Y., and I. Tsvankin, 2006, Plane-wave propagation in attenuative transversely isotropic media: Geophysics, **71**, no. 2, T17–T30, doi: 10.1190/1.2187792.